Journal of Hazardous Materials 203–204 (2012) 363–369

Contents lists available at SciVerse ScienceDirect

Journal of Hazardous Materials

journal homepage: www.elsevier.com/locate/jhazmat

Hierarchical architectures TiO_2: Pollen-inducted synthesis, remarkable crystalline-phase stability, tunable size, and reused photo-catalysis

Lingling Dou[a], Lishuang Gao[a], Xiaohui Yang[b,c], Xiuqin Song[a,*]

[a] College of Chemistry and Materials Science, Hebei Normal University, Shijiazhuang 050016, PR China
[b] Institute of Coal Chemistry, Chinese Academy of Science, Taiyuan 030001, PR China
[c] Shijiazhuang University, Shijiazhuang 050801, PR China

ARTICLE INFO

Article history:
Received 22 September 2011
Received in revised form
11 December 2011
Accepted 15 December 2011
Available online 23 December 2011

Keywords:
TiO_2
Hierarchical architectures
Pollen-inducing
Crystalline-phase stability
Reused photo-catalysis

ABSTRACT

TiO_2 with hierarchical architectures, tunable crystalline phase and thermal stability is successfully fabricated on a large scale through a facile hydrolysis process of $TiCl_4$ combining with inducing of pollen. The structure of the as-prepared TiO_2 is characterized by X-ray diffraction, Raman spectroscopy, infrared spectra, and scanning electron microscopy. The experimental results indicate that different phases (anatase, rutile or mixed crystallite) of TiO_2 can be synthesized by controlling the experimental conditions. The pure phase of rutile or anatase can be obtained at 100 °C, while the pure phase of anatase can be retained after being annealed at 900 °C. The hierarchical structures TiO_2 are constitute through self-assembly of nanoparticles or nanorods TiO_2, which exhibit high and reused photo-catalytic properties for degradation of methylene blue.

1. Introduction

TiO_2 is one of the most widely investigated materials for its photo-catalytic properties, including the photo-catalytic degradation of organic pollutants [1–4], photo-catalytic hydrogen generation [5,6] and selective photo-catalytic oxidation [7,8]. In any case, the properties and operational performance of TiO_2 depend on its crystal phase, morphology, size and architecture. For this reason, many attentions have been paid to the assembling process of hierarchical structures TiO_2 with controllable morphology and architectures by multi-level structure design. It has been demonstrated that many hierarchical structures, such as TiO_2, hematite and other metal oxides, applied in water treatment were very efficient [9–12]. The hierarchical structures possess good light-scattering properties and are expected to provide more efficient light harvesting. There have been extensive studies exploring approaches for synthesis of hierarchical structures TiO_2, including template method [13–16], hydrothermal or alcohol-thermal process [17–23]. Although the above methods are all effective and have their own irreplaceable advantage, they usually require more rigor conditions, expensive raw materials or special additives to complete the assembly process. Moreover, hierarchical structures with tunable crystalline phase are generally more difficult to get.

Different from conventional methods for hierarchical materials, herein we report a facile hydrolysis process of $TiCl_4$ with pollen as inducer for synthesis of TiO_2. Pollen is a kind of natural products and very easily to harvest and store. Besides, the pollen grains are uniform in particle size, with high surface area, and have species-specific morphologies which are often highly elaborate and complex in surface morphology. Hall et al. used pollen as a template to produce porous silica, calcium phosphate, and calcium carbonate microspheres in aqueous reaction solutions [24]. However, they synthesized titanium with pollen only in isopropoxide solutions [25]. In this work, we develop a simple pollen-inducing (instead of template) approach for fabricating hierarchical structures TiO_2 in pure water. The preparation conditions are much milder and simpler than those of conventional methods. The obtained hierarchical TiO_2 shows three interesting hierarchical morphology, tunable crystal phase structures (rutile, anatase and any composition mixture phases), remarkable crystalline phase stability, and higher reused photo-catalytic activity.

2. Experimental procedures

2.1. Preparation of hierarchical architectures TiO_2

In a typical process, the mixture of hydrochloric acid and deionized water were stirred for 30 min to form stable solution A. A designed amount of $TiCl_4$ was added drop-wise into solution A with stirring to form stable solution B. An amount of sinicus pollen was

* Corresponding author. Tel.: +86 031186268016; fax: +86 031186268016.
E-mail address: xiuqinsong@gmail.com (X. Q. Song).

0304-3894/$ – see front matter © 2011 Elsevier B.V. All rights reserved.
doi:10.1016/j.jhazmat.2011.12.043

dissolved in 15 ml of de-ionized water with stirring and then added into solution B. The ultimate solution was put into the water bath of 100 °C for 8 h. After the ultimate solution aged at room temperature for 12 h, the precipitates were filtered, washed with deionized water and then ethanol for several times and dried at 100 °C. Finally, the dried samples were calcined at 500, 700, 900 and 1100 °C for 2 h, respectively.

2.2. Characterization

Scanning electron microscopy (SEM) measurements were performed with a Hitachi S-4800 microscope. An X-ray diffraction (XRD) study was carried out using a Bruker D8 Advance X-ray diffractometer with Cu Ka radiation (λ = 1.5418 Å). Raman measurements were performed with a Jobin Yvon HR 800 micro-Raman spectrometer at 457.9 nm. Infrared spectra (IR) measurements were carried out on a Shimadu FIRE-8900 Fourier transform infrared spectrophotometer.

2.3. Photo-catalytic activity measurement

The photo-degradation of methylene blue was carried out in an aqueous solution at room temperature under UV light irradiation. A 20 W tube-like UV lamp was used as light source. In a typical experiment, 20 mg photo-catalyst was dispersed in 100 ml methylene blue solution (20 mg l^{-1}). The suspension was stirred magnetically 0.5 h in the dark in order to reach adsorption equilibrium. At the given time intervals, about 5 ml of the suspension was taken from the reaction beaker for the analysis of methylene blue concentration after centrifuging. The photo-catalytic activities of the samples were evaluated by measuring the absorbance of aqueous methylene blue solution at 662 nm as a function of irradiation time with a UV–vis spectrophotometer (VIS-7220). To demonstrate the stability of the photo-catalysts, we recycled the used hierarchical architectures TiO_2. Every experiment was repeated at least three times, and the average (with RSD less than 5% for three repeated results) was used as the final results. The degradation rate (%) was evaluated by the following equation:

$$D = \left[\frac{C_0 - C_t}{C_0}\right] \times 100\% \quad (1)$$

where D is degradation rate, C_0 and C_t are the concentrations of the methylene blue solution at UV irradiation time 0 and t, respectively.

3. Results and discussion

3.1. Structure of the hierarchical architectures TiO_2

In general, the crystal phase and crystallization of TiO_2 depend on the calcinations temperature. Anatase is the main phase of TiO_2 at low temperature and rutile is the final phase after being calcined at high temperature [26]. However, some novel results about the crystallization, crystal phase and stability of TiO_2 are obtained in the present study because of the inducing of pollen.

3.1.1. Crystallization temperature and high thermal stability of anatase TiO_2

The experimental results show that the acquired TiO_2 particles consist of anatase and rutile in the absence of pollen at 500 °C, which change to pure rutile at high temperatures. This traditional phase transition characteristics can vary with additional dosage of pollen. Fig. 1 shows the XRD patterns of hierarchical architecture TiO_2 obtained using 0.9 g/10 ml (reaction system) pollen at different calcination temperatures. It clearly shows that the tetragonal anatase phase TiO_2 from 100 °C to 900 °C can be observed and indexed as (1 0 1), (0 0 4), (2 0 0), (1 0 5), and (2 1 1), respectively

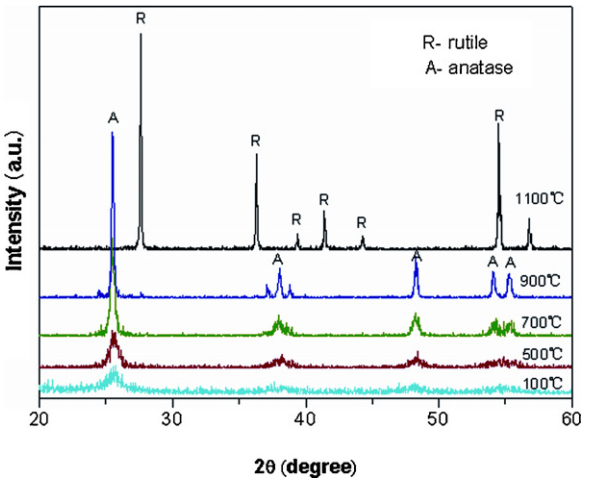

Fig. 1. XRD patterns of TiO_2 with different calcination temperatures.

(JCPDS, No.21-1272). Obviously, it is unusual to obtain crystallization of anatase TiO_2 at such a low temperature for atmospheric pressure hydrolysis reaction system [27]. With increasing calcination temperatures, the crystallinity of TiO_2 is improved obviously, and crystallization process finishes at 500 °C. It is noticeable that the pure anatase phase can be maintained at temperatures up to 900 °C, which is much higher than the reported values [28,29]. When the calcination temperature exceeds 900 °C, the anatase-to-rutile phase transition begins and the main phase rutile is obtained at 1100 °C. Detailed analysis of the peak broadening of the (1 0 1) reflection of anatase TiO_2 using the Scherrer equation indicates an average crystal size 17.6–56.6 nm for different temperature (from 100 °C to 900 °C). It illustrates that these hierarchical anatase TiO_2 architectures are composed of nanocrystal subunits. The above results should be attributed to the induction of pollen.

Raman spectroscopy, which is very sensitive to the crystallinity and microstructure of materials, is usually used to unambiguously discriminate the local order characteristics of TiO_2. In order to further confirm the high crystallinity of the obtained TiO_2, Raman detection was carried out. Fig. 2 shows the Raman spectra of hierarchical TiO_2 with different calcination temperatures. Under a calcination temperature of 900 °C, it can be observed clearly that the five high intensity Raman peaks at 149, 199, 393, 513, and 639 cm^{-1} can be ascribed to E_g, E_g, B_{1g}, A_{1g} (B_{1g}), and E_g modes, respectively. These modes are characteristics of the anatase TiO_2 [30]. Besides, the intensity of Raman peaks increases with the

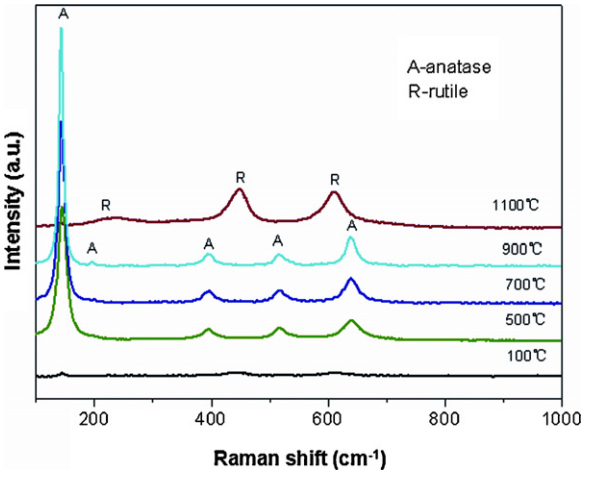

Fig. 2. Raman spectra of TiO_2 with different calcinations temperatures.

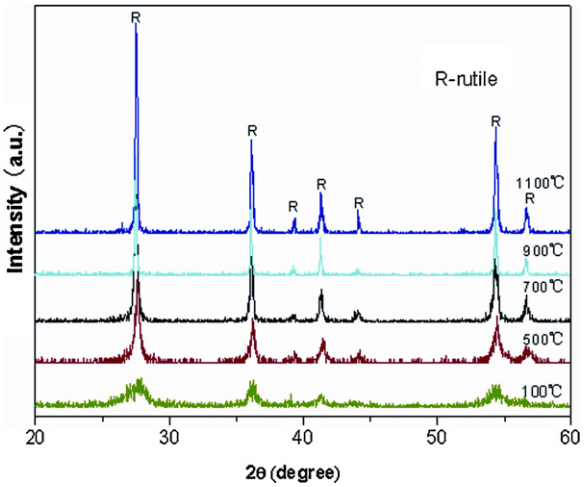

Fig. 3. XRD patterns of TiO_2 with different calcination temperatures.

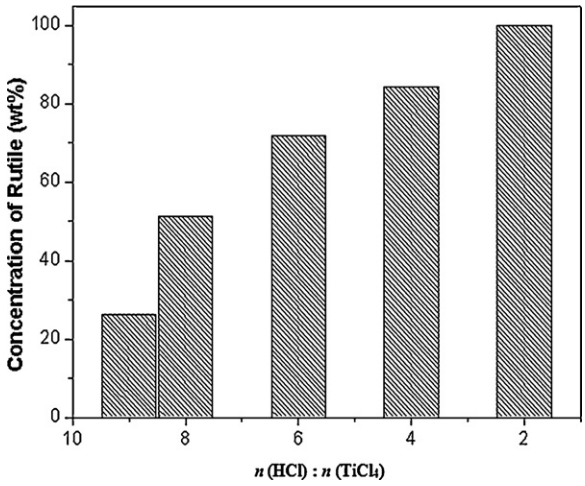

Fig. 4. The content of rutile TiO_2 with different mass ratio of $TiCl_4$ to HCl.

increase of calcination temperature, suggesting the improvement of crystallinity of anatase, which is in good agreement with the XRD results. When the calcination temperature reaches 1100 °C, four Raman peaks at 143, 244, 442, and 609 cm^{-1} can be observed and ascribed to B_{1g}, multi-photon process, E_g, and A_{1g} modes respectively, which are characteristics of the rutile TiO_2. These results are well consistent with the XRD characterization.

3.1.2. Crystallization and stability of rutile TiO_2

It is well-known that rutile is the most thermodynamically stable phase of TiO_2, and it is commonly prepared by calcination of anatase TiO_2 at high temperature. In this work, the pure crystallization phase of rutile TiO_2 can be obtained at 100 °C by controlling the mass ratio of $TiCl_4$ and HCl at 1:2 in the presence of pollen (0.9 g/10 ml). XRD spectra of the as-prepared rutile TiO_2 are shown in Fig. 3. The peaks assignable to rutile are those at $2\theta = 27.5°$, 36.5°, 41.0°, 54.1° and 56.5°, respectively (JCPDS, No.21-1276), none anatase peaks is observed, indicating the phase-pure rutile. The crystal process of rutile TiO_2 finishes at 500 °C. The particle sizes are calculated to be 8.84 nm and 59.6 nm for the non-calcinated and calcinated 1100 °C samples, respectively. It can be proved that these rutile TiO_2 hierarchical architectures are all composed of nano-size subunits.

3.1.3. Constitution of mixed crystallite TiO_2

Fig. 4 shows the content of rutile of the hierarchical architectures TiO_2 calcined at 500 °C with different molar ratio of $TiCl_4$ to HCl. It is found that the ratio of $TiCl_4$ to HCl influences of the crystal phase of products. The content of rutile increases with the decrease of solution pH values in the presence of 0.9 g/10 ml of pollen. Thus, through changing the content of HCl in reaction systems, we can effectively control the crystal phase structure of the products.

3.2. Morphology of hierarchical architectures TiO_2

As shown in Fig. 5, the original morphology of sinicus pollen used in the experiment is a spinous spherical shape with the diameter ranging from 20 μm to 30 μm. It is found that the TiO_2 particles were irregular and distribute as reunite state in the absence of pollen, as shown in Fig. 6. When the contents of pollen exceeded 0.3 g/10 ml (reaction system), the morphology of products is determined not only by pollen, but also by the contents of HCl of the reaction system. Fig. 7 shows the typical SEM images of as-prepared TiO_2 with different $TiCl_4$ to HCl molar ratio when the dosage of pollen remains unchanged. Certainly, shapes of as-synthesized TiO_2

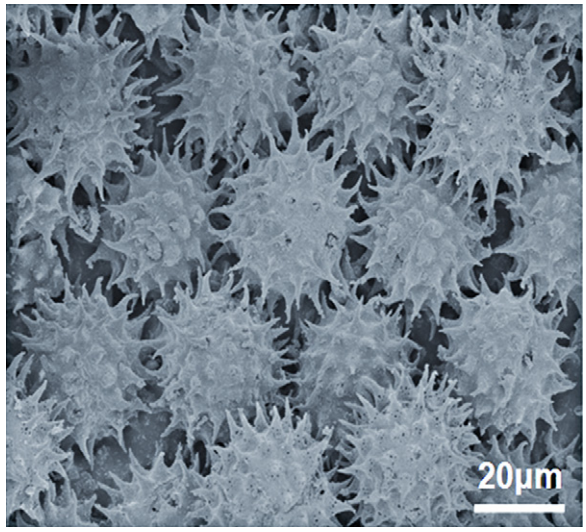

Fig. 5. The SEM images of the original pollen.

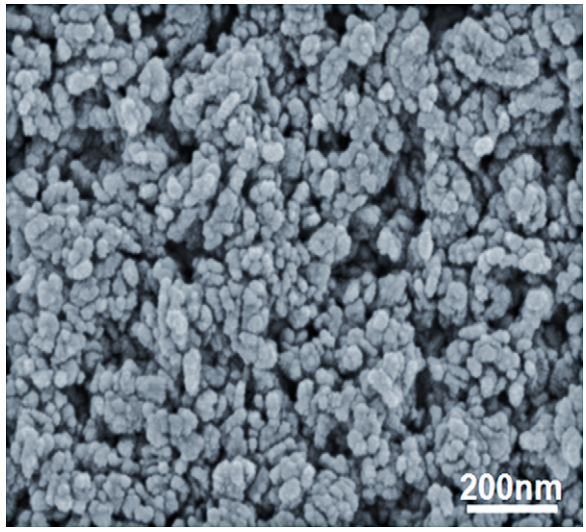

Fig. 6. The SEM images of TiO_2 in the absence of pollen.

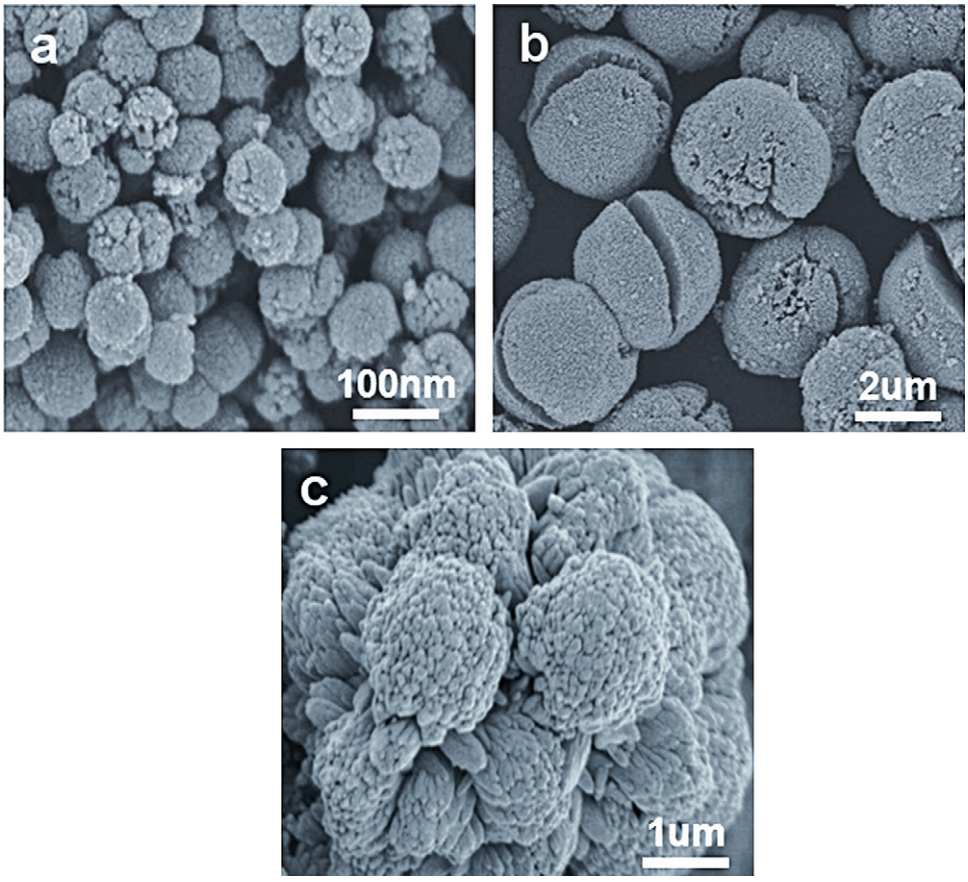

Fig. 7. The low magnification SEM images of TiO_2 with different mass ratio of $TiCl_4$ to HCl ((a) 1:8, (b) 1:4, (c) 1:2).

are irregular without pollen. When the mass ratio of $TiCl_4$ to HCl is 1:8, it can be observed in Fig. 7(a) that the samples consist of nano-size spherical particles, which are consisted of smaller nanoparticles with diameter of about 10 nm. When the $TiCl_4$ to HCl ratio is 1:4, morphology of TiO_2 is microspheres with the diameter ~3 μm, as shown in Fig. 7(b). Fig. 7(c) shows the image of TiO_2 with full-blown cauliflower shape when the $TiCl_4$ to HCl ratio is 1:2.

The high magnification SEM images of the microspheres and full-blown cauliflower shape are shown in Fig. 8. Microspheres are made up nanorods in an order arranging with diameter of about 10 nm (Fig. 8(a)). Fig. 8(b) shows that the hierarchical architecture grows more abundant under such circumstances. The first layer consists of nanorods with diameter of about 30 nm. These further assemble to clusters-like microspheres with diameter of about 1 μm, which are an integral component of the second layer. The third layer with full-blown cauliflower shape is composed of these microspheres.

We can come to a conclusion that pollen can induce the generation of regular shape TiO_2. At the same time, through controlling the pH of the reaction system, many kinds of hierarchical architecture TiO_2 can be achieved. Nano-size TiO_2 building blocks are self-assembly into micro-scale TiO_2 with controllable architectures. Therefore, the recycled utilization of the stable hierarchical architecture TiO_2 is possible and its stability in treating organic contaminated water is satisfactory.

The typical SAXRD patterns of hierarchical architecture TiO_2 with different calcination temperatures are shown in Fig. 9. At least one resolved peaks are observed. It may indicate that there are higher ordered porous in the as-prepared hierarchical TiO_2.

3.3. Discussion on formation mechanism of hierarchical TiO_2

The original morphology of sinicus pollen used in the present investigation is spinous spherical-shaped with the diameter of 20–30 μm. As-prepared TiO_2 does not copy the pollen shape instead of forming different kinds of hierarchical architecture. This indicates that the role of pollen is not a simple template, but some compositions or function groups of pollen played an induction role for the nucleation and growth of TiO_2.

In order to understand the interactions of pollen and TiO_2 precursors, the FT-IR spectra of the original sinicus pollen, intermediary product and the ultimate product calcined at 500 °C are measured, as shown in Fig. 10. It is found that the IR curves of pollen used in the experiment are in accord with the characters of usual pollen [31]. The position of the main peak includes the broad bands around 3400 cm^{-1}, which is corresponding to the stretching vibration of hydroxyl. The peak around 2920 cm^{-1} and the shoulder peak nearby are corresponding to the asymmetric stretching vibration of methylene. The peaks at 1640 and 1550 cm^{-1} are corresponding to vibration of amino I and amino II in protein. The peak at 1060 cm^{-1} is corresponding to the stretching vibration of C–O [32]. It is demonstrated there are organic frame and rich organic functional groups in the pollen. Comparing Fig. 10(b) with (a), we can find that these peaks almost disappear but the intensity of vibration of amino I and amino II in protein becomes weaker and shifts a little. Residual amino is perhaps the key function groups for inducing nucleation and growth of hierarchical architectures TiO_2. The shift of peak shows the interaction between the pollen and TiO_2 precursors. The disappearance of the absorption bands of all organic function groups (Fig. 10(c)) illustrates the pollen structure completely disappeared after treatment at 500 °C.

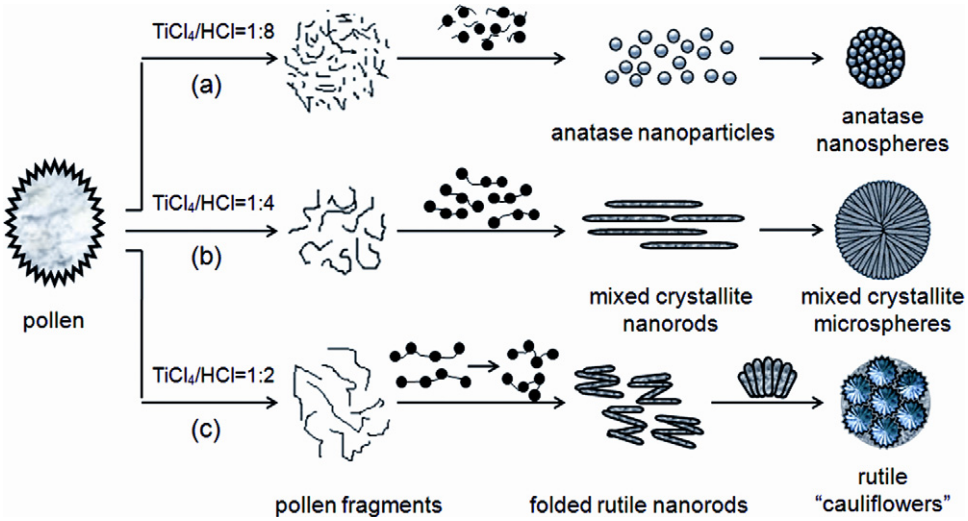

Scheme 1. Schematic illustration of hierarchical architectures TiO_2 formation.

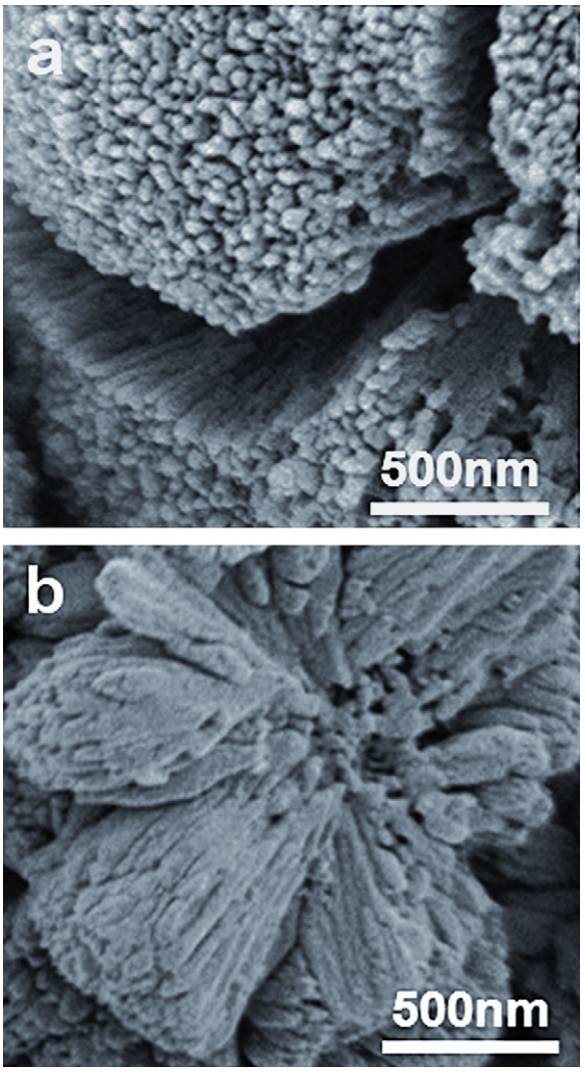

Fig. 8. The high magnification SEM images of TiO_2 with different mass ratio of $TiCl_4$ to HCl ((a) 1:4, (b) 1:2).

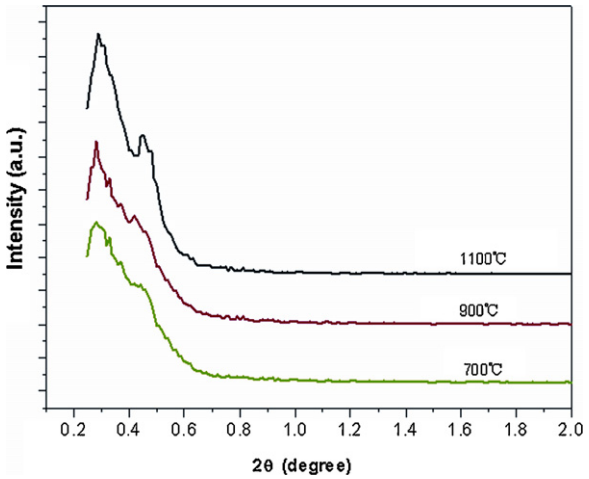

Fig. 9. SAXRD patterns of TiO_2 with different calcination.

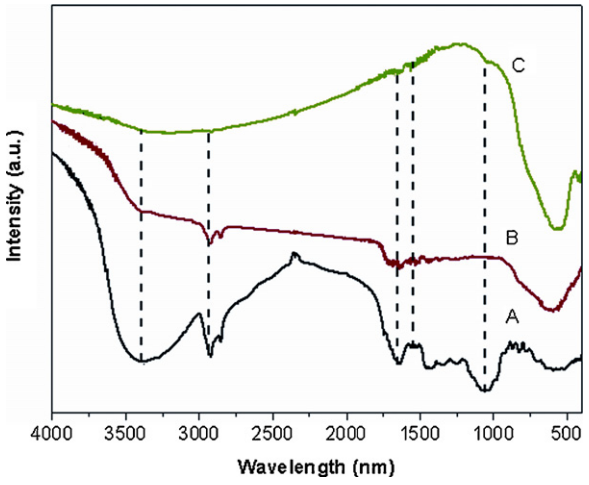

Fig. 10. Evolution of the FT-IR spectra of the original pollen (a), intermediary products (b), products calcined at 500 °C (c).

The mechanism model for the formation of hierarchical structure of TiO_2 is tentatively proposed as shown in Scheme 1. The whole process can be described.

The reaction system exhibits strong acidity as adding HCl, and acidity continuous to strengthen with $TiCl_4$ hydrolysis process. Under strong acidic conditions, the structure of pollen will be destroyed, and the complete skeleton will be snipped into fragments. The some organic components (e.g. amino) of pollen fragments can induce the nucleation of TiO_2 and formation of TiO_2 nanoparticles in the way of region-selectivity. This way of "selective regional nuclear" brings together into regular morphology of products and no scattering TiO_2.

(a) In strong acid medium (the mole ratio of $TiCl_4$ to HCl is 1:8), pollen is destroyed seriously, there are a great number of small volume pollen fragments in the system, which caused anatase crystals can only exist as nanometer sized "small" crystals. These nanoparticles can be gathered into nanospheres, which maintain the anatase structure. The phase transition from anatase to rutile can only happen at high temperature (>900 °C) because displacement of atoms in these nanoparticles is limited. Here, the induction of pollen and resulting steric hindrance contribute to the lower crystallization temperature and higher thermal stability of anatase TiO_2.
(b) When the acid strength is weakened (1:2 < $TiCl_4$:HCl < 1:8), pollen fragments become bigger in size or volume. The nucleation points increase in the same fragments. In the process of crystal growth, neighboring nano-particles are assembled into nanorods based on the so-called oriented attachment mechanism. The immediate results of the oriented attachment create the transformation of anatase to rutile and obtain mixed crystallite nanorods. The nanorods aggregate further into microspheres.
(c) In lower acidity medium (the ratio of $TiCl_4$ to HCl is 1:2), pollen fragments have much longer in size or volume. TiO_2 nanoparticles achieve oriented attachment over a greater range. The shape of as-products is long chain-like, which fold into a few nanorods clusters and subsequent cauliflowers for stabilization. The pure rutile TiO_2 can be obtained because of completely oriented attachment at large scale.

To sum up, the role of pollen is to induce the nucleation of TiO_2 and formation of TiO_2 nanoparticles in the way of region-selectivity, instead of hard template or as seed for precursor solution. The assembly mode of TiO_2 nanoparticles is oriented but circumscribed by the size or volume of pollen fragments. All the obtained hierarchical structures of TiO_2 are with regular morphology. No scattering TiO_2 is obtained. On the other hand, the oriented attachment of TiO_2 nanoparticles accomplishes in the way of aggregation. As a result, this system has not yet reached the mesocrystal state.

3.4. Photo-catalytic performance

Fig. 11 shows the time-dependent degradation ratio using the obtained hierarchical architectures samples and commercial P_{25} TiO_2 as photo-catalysts. From the degradation ratio, we can clearly see that the anatase hierarchical architectures TiO_2 exhibit best activity. About 98.7% of methylene blue molecules were degraded after UV irradiation for 1 h for anatase sample, which is higher than that of P_{25}. The relative photo-catalytic activity of the catalysts decreases in the order of anatase > P_{25} > mixed crystallite > rutile. The activity levels of irregular TiO_2 particles acquired in the absence of pollen are the lowest and TiO_2 particles are hard to recycle them.

Specifically, these hierarchical structures can be readily separated by filtration or sedimentation after reaction because of their

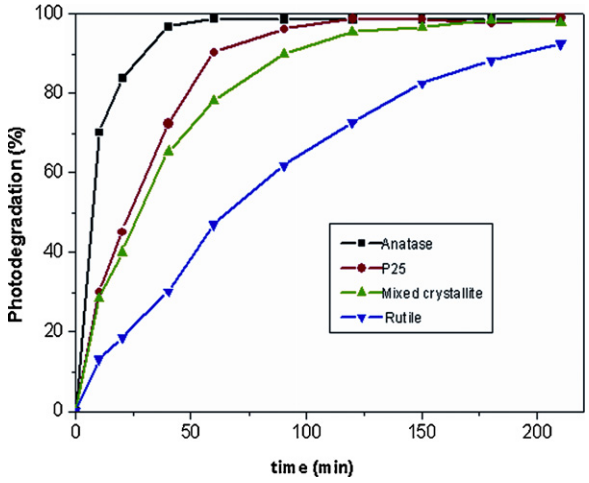

Fig. 11. Time profiles of photo-catalytic degradation of methylene blue for different catalysts calcined at 500 °C.

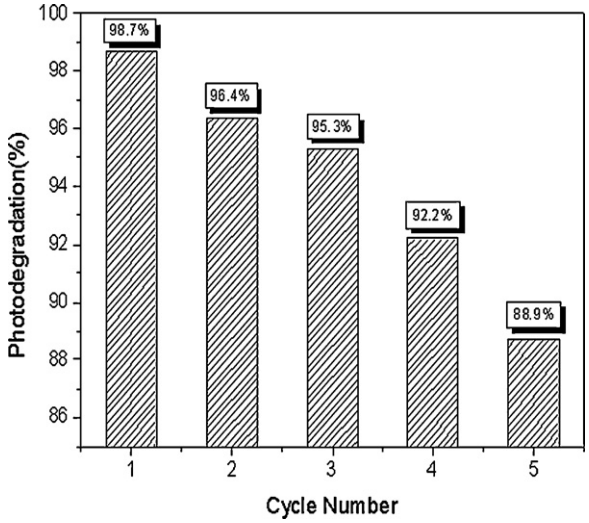

Fig. 12. The recycling of anatase TiO_2 for photodegradation of methylene blue.

nano-/micro architectures. In addition, stability is very important for recycling of catalysts in practical applications. To prove the possibility of recyclability of the hierarchical structures TiO_2, cycle experiments were performed. The typical recycled experiments results of anatase TiO_2 are shown in Fig. 12. We can clearly see that the ratio of photo-degradation is remained at more than 80 percent of the high level even recycle five times. Therefore, the recyclability of the stable hierarchical architectures TiO_2 is possible and its stability in treating organic contaminated water is satisfactory.

4. Conclusion

In summary, we develop a simple pollen-inducing (instead of hard template) approach, which is different from conventional methods, for the fabrication of hierarchical structures TiO_2 on a large scale. The three kinds of hierarchical TiO_2 micro-sized materials are constructed by the self-assembly of nanoparticles or nanorods of TiO_2. These hierarchical TiO_2 microspheres show the interesting hierarchical morphology, the tunable crystal phase structures (rutile, anatase and any composition mixture phases) and remarkable crystalline-phase stability. It is demonstrated that the obtained anatase TiO_2 exhibits higher and reused catalytic activity than that of Degussa P_{25} for degradation of methylene blue

under UV irradiation. These hierarchical TiO_2 microspheres should have great applications in photo-catalysis, catalysis, solar cells, separation and purification processes. This study provides an example for better understanding the formation mechanism of other inorganic hierarchical materials in the presence of pollen. We believe that the present work will open up systematically explore ways to fabricate hierarchical structures and thus find use in a variety of applications.

Acknowledgments

This work was supported by NSFC (No. 21077031) and Hebei Natural Science Foundation (No. E2008000189).

References

[1] A.L. Linsebigler, G.Q. Lu, J.T. Yates, Photocatalysis on TiO_2 surfaces: principles, mechanisms, and selected results, Chem. Rev. 95 (1995) 735–758.
[2] X.B. Chen, S.S. Mao, Titanium dioxide nanomaterials: synthesis, properties, modification, and applications, Chem. Rev. 107 (2007) 2891–2959.
[3] D.S. Wang, L.B. Xiao, Q.Z. Luo, X.Y. Li, J. An, Y.D. Duan, Highly efficient visible light TiO_2 photocatalyst prepared by sol–gel method at temperatures lower than 300 °C, J. Hazard. Mater. 192 (2011) 150–159.
[4] A.M. Hu, X. Zhang, K.D. Oakesb, P. Peng, Y.N. Zhou, M.R. Servos, Hydrothermal growth of free standing TiO_2 nanowire membranes for photocatalytic degradation of pharmaceuticals, J. Hazard. Mater. 189 (2011) 278–285.
[5] F.Y. Wen, J.H. Yang, X. Zong, Y. Ma, Q. Xu, B.J. Ma, C. Li, Photocatalytic hydrogen production utilizing solar energy, Prog. Chem. 21 (2009) 2285–2302.
[6] X.B. Chen, S.H. Shen, L.J. Guo, S.S. Mao, Semiconductor-based photocatalytic hydrogen generation, Chem. Rev. 110 (2010) 6503–6570.
[7] S. Yurdakal, G. Palmisano, V. Loddo, V. Augugliaro, L. Palmisano, Nanostructured rutile TiO_2 for selective photocatalytic oxidation of aromatic alcohols to aldehydes in water, J. Am. Chem. Soc. 130 (2008) 1568–1569.
[8] X.J. Lang, H.W. Ji, C.C. Chen, W.H. Ma, J.C. Zhao, Selective formation of imines by aerobic photocatalytic oxidation of amines on TiO_2, Angew. Chem. Int. Ed. 50 (2011) 3934–3937.
[9] J.H. Pan, X.W. Zhang, A.J.H. Du, D.D. Sun, J.O. Leckie, Self etching reconstruction of hierarchically mesoporous F–TiO_2 hollow microspherical photocatalyst for concurrent membrane water purifications, J. Am. Chem. Soc. 130 (2008) 11256–11257.
[10] X. Huang, J.G. Guan, Z.D. Xiao, G.X. Tong, F.Z. Mou, X.A Fan, Flower-like porous hematite nanoarchitectures achieved by complexation-mediated oxidation–hydrolysis reaction, J. Colloid Interface Sci. 357 (2011) 36–45.
[11] G.X. Tong, J.G. Guan, Q.J. Zhang, Goethite hierarchical nanostructures: glucose-assisted synthesis, chemical conversion into hematite with tailored crystallization, texture characteristics, and excellent catalytic properties, Mater. Chem. Phys. 127 (2011) 371–378.
[12] G.X. Tong, J.G. Guan, Z.D. Xiao, X. Huang, Y. Guan, In-situ generated gas bubble-assisted modulation of the morphologies, photocatalytic and magnetic properties of ferric oxide nanostructures synthesized by thermal decomposition of iron nitrate, J. Nanopart. Res. 12 (2010) 3025–3037.
[13] X.X. Li, Y.J. Xiong, Z.Q. Li, Y. Xie, Large-scale fabrication of TiO_2 hierarchical hollow spheres, Inorg. Chem. 45 (2006) 3493–3495.
[14] J.G. Yu, W. Liu, H.G. Yu, A one-pot approach to hierarchically nanoporous titania hollow microspheres with high photocatalytic activity, Cryst. Growth Des. 8 (2008) 930–934.
[15] Y. Li, X.S. Fang, N. Koshizaki, T. Sasaki, L. Li, S.Y. Gao, Y. Shimizu, Y. Bando, D. Golberg, Periodic TiO_2 nanorod arrays with hexagonal nonclose-packed arrangements: excellent field emitters by parameter optimization, Adv. Funct. Mater. 19 (2009) 2467–2473.
[16] X.F. Li, T.X. Fan, H. Zhou, S.K. Chow, W. Zhang, D. Zhang, Q.X. Guo, H. Ogawa, Enhanced light-harvesting and photocatalytic properties in morph-TiO_2 from green-leaf biotemplates, Adv. Funct. Mater. 19 (2009) 45–56.
[17] Y.F. Tang, L. Yang, J.Z. Chen, Z. Qiu, Facile fabrication of hierarchical hollow microspheres assembled by titanate nanotubes, Langmuir 26 (2010) 10111–10114.
[18] Z.K. Zheng, B.B. Huang, X.Y. Qin, X.Y. Zhang, Y. Dai, Strategic synthesis of hierarchical TiO_2 microspheres with enhanced photocatalytic activity, Chem. Eur. J. 16 (2010) 11266–11270.
[19] W.B. Hu, L.P. Li, W.M. Tong, G.S. Li, T.J. Yan, Tailoring the nanoscale boundary cavities in rutile TiO_2 hierarchical microspheres for giant dielectric performance, J. Mater. Chem. 20 (2010) 8659–8667.
[20] J.F. Ye, W. Liu, J.G. Cai, S. Chen, X.W. Zhao, H.H. Zhou, L.M. Qi, Nanoporous anatase TiO_2 mesocrystals: additive-free synthesis, remarkable crystalline phase stability, and improved lithium insertion behavior, J. Am. Chem. Soc. 133 (2011) 933–940.
[21] S.S. Mali, C.A. Betty, P.N. Bhosale, P.S. Patil, Hydrothermal synthesis of rutile TiO_2 with hierarchical microspheres and their characterization, Cryst. Eng. Commun. 13 (2011) 6349–6351.
[22] S.S. Mali, S.K. Desai, D.S. Dalavi, C.A. Betty, P.N. Bhosale, P.S. Patil, CdS-sensitized TiO_2 nanocorals: hydrothermal synthesis, characterization, application, Photochem. Photobiol. Sci. 10 (2011) 1652–1658.
[23] S.S. Mali, P.S. Shinde, C.A. Betty, P.N. Bhosale, W.J. Lee, P.S. Patil, Nanocoral architecture of TiO_2 by hydrothermal process: synthesis and characterization, Appl. Surf. Sci. 257 (2011) 9737–9746.
[24] S.R.Hall, H. Bolger, S. Mann, Morphosynthesis of complex inorganic forms using pollen grain templates, Chem. Commun. 278 (2003) 4–2785.
[25] S.R. Hall, V.M. Swinerd, F.N. Newby, A.M. Collins, S. Mann, Fabrication of porous titania (Brookite) microparticles with complex morphology by sol–gel replication of pollen grains, Chem. Mater. 18 (2006) 598–600.
[26] W.B. Yue, C. Randorn, P.S. Attidekou, Z.X Su, J.T.S. Irvine, W.Z. Zhou, Syntheses, Li insertion, and photoactivity of mesoporous crystalline TiO_2, Adv. Funct. Mater. 19 (2009) 2826–2833.
[27] C. Wang, Z.X. Deng, Y.D. Li, The synthesis of nanocrystalline anatase and rutile titania in mixed organic media, Inorg. Chem. 40 (2001) 5210–5214.
[28] M. Fernández-García, A. Martínez-Arias, J.C. Hanson, J.A. Rodriguez, Nanostructured oxides in chemistry: characterization and properties, Chem. Rev. 104 (2004) 4063–4104.
[29] W. Zhou, F.F. Sun, K. Pan, G.H. Tian, B.J. Jiang, Z.Y. Ren, C.G. Tian, H.G. Fu, Well-ordered large-pore mesoporous anatase TiO_2 with remarkably high thermal stability and improved crystallinity: preparation, characterization, and photocatalytic performance, Adv. Funct. Mater. 21 (2011) 1922–1930.
[30] H. Chang, P.J. Huang, Thermo-Raman studies on anatase and rutile, J. Raman Spectrosc. 29 (1998) 97–102.
[31] E. Gottardini, S. Rossi, F. Cristofolini, L. Benedetti, Use of Fourier transform infrared (FT-IR) spectroscopy as a tool for pollen, Aerobiologia 23 (2007) 211–219.
[32] F. Cao, D.X. Li, Morphology-controlled synthesis of SiO_2 hollow microspheres using pollen grain as a biotemplate, Biomed. Mater. 4 (2009) 1–6.